AIAA JOURNAL
Vol. 35, No. 1, January 1997

NASA Langley Mach 6 Quiet Wind-Tunnel Performance

Alan E. Blanchard*
Old Dominion University, Norfolk, Virginia 23529
Jason T. Lachowicz†
North Carolina State University, Raleigh, North Carolina 27695-7910
and
Stephen P. Wilkinson‡
NASA Langley Research Center, Hampton, Virginia 23681-0001

The flow in the NASA Langley Mach 6 quiet wind tunnel has been investigated to quantify the effectiveness of laminar-flow control techniques used to delay transition of the nozzle-wall boundary layer. The results of this investigation include an assessment of the mean and unsteady nozzle flow to define the quiet core length, and hence performance, over the operating range of the facility. A large, uniform region of Mach 5.91 flow was documented for a variety of unit Reynolds numbers. By using a prototype constant-voltage anemometer to measure the unsteady flowfield, acoustic radiation patterns from the transitional nozzle-wall boundary layers were mapped. These disturbances originating at the irregular edge of the transitional nozzle-wall boundary layer were shown to follow Mach lines into the test section of the nozzle, thereby limiting the length of the quiet core. With a virtual origin downstream of the nozzle throat, a Reynolds number dependency was found for the amplitudes of the acoustic radiation. The spectral evolution of noisy flow in the quiet tunnel was shown, and measurable freestream disturbances, outside the region of quiet flow, were found to be qualitatively similar to those documented for conventional high-speed tunnels. In sum, the laminar-flow control techniques used to delay nozzle-wall boundary layer transition in the Mach 6 nozzle test chamber facility have succeeded in producing a substantial region of quiet flow suitable for high-speed boundary layer stability research.

Nomenclature

M = Mach number
N_G = N-factor (integrated growth rate) of Görtler instability
Re_V = freestream Reynolds number based on V, $(\rho U V/\mu)_\infty$
Re_{VT} = freestream Reynolds number based on VT, $(\rho U VT/\mu)_\infty$
Re_X = freestream Reynolds number based on X, $(\rho U X/\mu)_\infty$
$Re_{\Delta X}$ = freestream Reynolds number based on ΔX, $(\rho U \Delta X/\mu)_\infty$
Re_∞ = freestream unit Reynolds number, $(\rho U/\mu)_\infty$ per m
rms = root mean square of fluctuating component of hot-wire signal
U = mean freestream velocity
V = downstream distance from the virtual origin, cm
VT = distance between the virtual origin and the location of nozzle-wall boundary layer transition, cm
X = downstream distance from nozzle throat, cm
x = distance from apex of test cone, cm
Y = transverse distance from nozzle centerline, cm
Z = vertical distance from nozzle centerline, cm
α = Mach angle, $\sin^{-1}(1/M)$
β = nozzle exit shock angle
ΔX = length of quiet test core, cm
μ = viscosity
ρ = density
∞ = freestream condition

Presented as Paper 96-0441 at the AIAA 34th Aerospace Sciences Meeting, Reno, NV, Jan. 15–19, 1996; received Feb. 21, 1996; revision received Oct. 3, 1996; accepted for publication Oct. 11, 1996; also published in *AIAA Journal on Disc*, Volume 2, Number 2.

*Graduate Research Assistant, Department of Mechanical Engineering.
†Graduate Research Assistant, Department of Mechanical and Aerospace Engineering; currently National Research Council Associate, NASA Langley Research Center, Hampton, VA 23681. Member AIAA.
‡Research Engineer, Flow Modeling and Control Branch. Senior Member AIAA.

Introduction

IT has been known for over 40 years that experimental, high-speed facility flows produce significant freestream disturbance fields[1–4] that complicate the comparison of experimental boundary layer stability data and theoretical predictions. These fields, which vary with tunnel design, perturb model boundary layers differently, producing conflicting results for similar models. To elucidate this point, variations in transition Reynolds number for cone and flat plate models in different high-speed wind tunnels ($3 < M < 8$) were correlated to wind-tunnel parameters 25 years ago.[5,6] This result confirmed the detrimental effect of freestream acoustic disturbances radiating from the turbulent boundary layers on the walls of the test section and established the need for low-disturbance, high-speed test facilities. Clearly, the key to designing a successful low-disturbance high-speed test facility lies in maximizing the extent of laminar flow over the walls of the test section. To this end, a 25-year research and development program at the NASA Langley Research Center has centered on applying laminar-flow control technology to high-speed wind tunnels, with the Mach 6 nozzle test chamber facility representing the latest contribution to this effort.

High-speed wind tunnels generate freestream disturbances in a variety of ways. Steady-state nonuniformities in the mean flow are caused by nozzle geometry imperfections and can be minimized by careful fabrication.[2] The unsteady freestream disturbances, however, are more involved and classically have been characterized as vorticity, entropy, and sound modes[7] generated in the settling chamber or nozzle.[1,2] Vorticity mode disturbances (turbulence) are generally negligible for hypersonic nozzles because of the large flow expansion from the settling chamber to the test section.[3,8] Entropy mode disturbances (temperature spottiness) are negligible if the heated flow has been mixed thoroughly before entering the test section.[2] The sound mode is the most significant source of high-speed noise and has many acoustic sources, including Mach wave radiation from turbulent boundary layers, shivering Mach waves

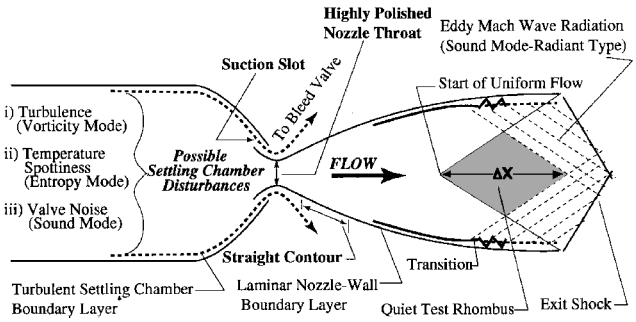

Fig. 1 Typical quiet tunnel and possible disturbance modes.

from surface irregularities, and sound wave propagation from the settling chamber.[1,2] Techniques have been developed to determine the amplitude[7] and convection velocity[3,4] of these acoustic sources via mode-diagram analysis of hot-wire data. In general, acoustic disturbances radiating from the turbulent tunnel wall boundary layer[3] are the dominant source of freestream disturbances in high-speed flow facilities.

Quiet tunnel technology developed and implemented at NASA Langley Research Center during the 1970s and 1980s maximizes the extent of laminar flow over the nozzle wall through a variety of laminar-flow control techniques (see Refs. 9–11). Certain elements are unique to a typical Langley-design quiet tunnel as shown in Fig. 1. They are 1) a suction slot upstream of the nozzle throat to bleed off the turbulent settling chamber boundary layer,[12] 2) a highly polished nozzle throat to minimize the transition-promoting effects of roughness,[13] and 3) a straight contour just downstream of the nozzle throat to delay the development of Görtler vortices.[14] Transition measurements obtained in a quiet tunnel environment show transition trends closer to that of free flight than do data from conventional tunnels[9] and confirm the effectiveness of quiet tunnels for high-speed stability and transition research.

In conjunction with the Langley program for hypersonic instability and transition research, a quiet Mach 6 facility was developed. This involved retrofitting a new quiet nozzle and settling chamber modifications to the Langley nozzle test chamber facility. The modified facility is commonly known as the Mach 6 nozzle test chamber facility or M6NTC. The nozzle flow was initially investigated in 1991 (Ref. 14) with an anemometry system highly susceptible to electronic noise before a replating process was discovered that has reduced surface oxidation potential and enhanced throat smoothness. An abbreviated investigation of the present facility flow is documented in Ref. 10; however, it is known that transition on the nozzle wall in the M6NTC is detectable from freestream measurements[11] and that the frequency content of the acoustic noise[10] follows typical trends for the disturbances in a conventional tunnel.[15]

The purpose of the present research is to investigate the M6NTC facility flow by using an anemometry system with much greater immunity to electronic noise (relative to previous research) to quantify the overall performance of the quiet tunnel and to demonstrate the effectiveness of the laminar-flow control measures used in the quiet tunnel design. An improved anemometry system has resulted in a better signal-to-noise ratio and greater frequency resolution of the fluctuating data compared to that used in Ref. 14 as well as enhanced spatial resolution due to improved probing techniques. In addition, detailed mean flow data show the uniformity of the mean flow in the M6NTC. Research conducted after the current investigation has shown conclusively the utility of the M6NTC facility for unique stability and transition measurements over conical configurations[16–19] in a low-freestream noise environment.

Description of Experimental Apparatus

The M6NTC, traversing mechanism location, and the coordinate system used is shown in Fig. 2. Because of the limited space between the nozzle exit, $X = 101.00$ cm, and the diffuser, traverses in the X direction are limited to 17.78 cm for the pitot surveys and to 20.32 cm for the hot-wire surveys. Thus, overlapping surveys with probes of various lengths were conducted to investigate the nozzle region of interest. Pitot surveys were also made for select Z planes. The

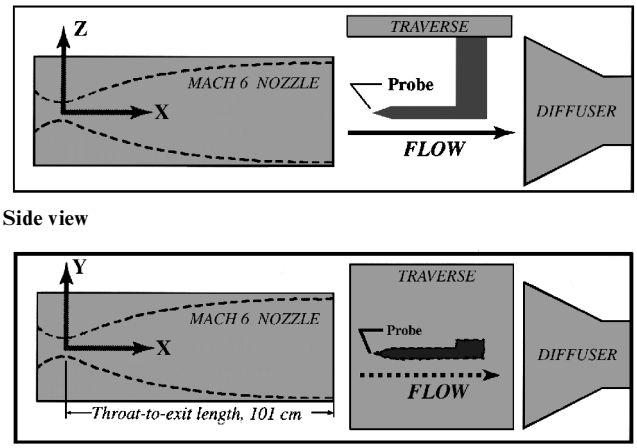

Fig. 2 Coordinate system, nozzle, and traverse mechanism (not to scale).

origin of the coordinate system is the throat of the nozzle with X increasing downstream.

For pitot surveys, a stainless steel tube (82.55 cm long and 1.27 cm outside diameter) with a tapered tip was used to support the pitot probe tubing. Stainless steel tubing (0.23 cm outside diameter and 0.15 cm inside diameter) was brazed into the tip of the structural tubing to form the pitot probe. Stagnation pressure and temperature were monitored at the settling chamber.

The Mach number was calculated by using the normal shock relations. These relations specify that the Mach number in front of the pitot tube shock is a function of the pitot tube and stagnation chamber pressures. The error in the Mach number was estimated to be ± 0.01 according to the uncertainty analysis of Kline and McClintock.[20]

For hot-wire surveys, a prototype constant-voltage anemometer (CVA) was used with single-wire hot-wire probes. Operation and theoretical discussions on the use of CVA are in the literature.[21,22] This particular CVA was observed to have better immunity to high-amplitude electromagnetic noise present in the laboratory than either constant-current or constant-temperature anemometers. (Note that the electronic features of the CVA that afforded the improved immunity were not investigated.) The sensing wire was oriented normal to the mean flow and in the X-Y plane. A spot welding technique was used to fix 2.54-μm-diam platinum-plated tungsten wires to the probe supports. The length of the sensing wire was on the order of 100 wire diameters. A series of three 1.27-cm (outside diameter) tubes of various lengths were fabricated to support the hot-wire probes. The CVA system had a bandwidth of about 400 kHz.

Unit Reynolds Number Selection

To select the Re_∞ range for investigation, a preliminary hot-wire investigation was conducted with the sensing wire fixed at the center of the nozzle exit as Re_∞ was varied. As shown in Fig. 3, the rms signal of the uncalibrated hot wire rose above the CVA noise level as Re_∞ approached 10.04×10^6/m with the M6NTC nozzle lip bleed valves open (BVO), which allows for removal of the settling chamber wall boundary layer. (All Re_∞ are estimated to be accurate to within $\pm 0.06 \times 10^6$/m.) With the bleed valves closed (BVC), the nozzle-wall boundary layer is fully turbulent and increasing Re_∞ produces only slight disturbance amplitude growth. These trends are consistent with an earlier investigation of the nozzle.[10]

For the purposes of the present investigation, quiet flow is defined by the absence of measurable unsteady flow disturbances. With BVO, there is a flat rms noise level from the CVA for $Re_\infty \leq 9.68 \times 10^6$/m that corresponds to the wind-off noise level of the CVA. This trend suggests that none of the disturbance modes, sound, entropy, or vorticity, have a significant, i.e., measurable, amplitude in the BVO case for $Re_\infty \leq 9.68 \times 10^6$/m. Because the entropy and vorticity modes as well as that portion of the sound mode associated with acoustic disturbances propagating from the settling chamber are generated upstream and are convected into the nozzle, the state of the bleed valves should have little effect on these modes

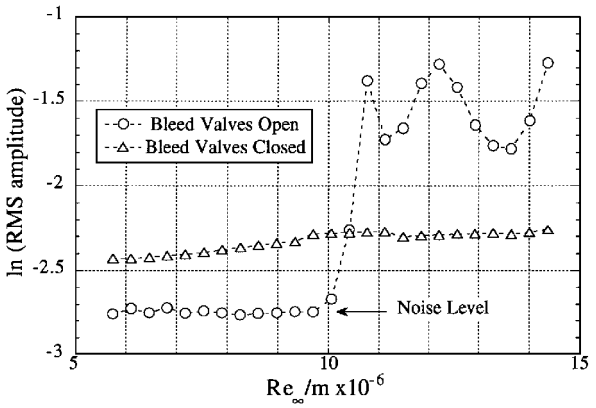

Fig. 3 Variation in hot-wire response with Re_∞ at $X = 101.0$ cm, $Y = Z = 0$.

at a fixed Re_∞. From comparison of the BVO and BVC cases for $Re_\infty < 9.68 \times 10^6$/m, the data in Fig. 3 suggest that the radiant sound mode dominates the BVC case. With BVC, the M6NTC behaves as a conventional tunnel with no region of quiet flow for the range of Re_∞ investigated.

In an earlier investigation of a Mach 5 quiet nozzle in the nozzle test chamber,[13] mode-diagram analysis of hot-wire data revealed an abrupt increase in the pressure fluctuation that typified the generation of the radiant sound mode (acoustic radiation). In that study, the abrupt increase in pressure fluctuations was associated with moving acoustic sources unique to a transitional/turbulent nozzle-wall boundary layer. It is believed that the sudden increase in rms amplitude for the BVO case for $Re_\infty > 9.68 \times 10^6$/m presented in Fig. 3 is likewise indicative of acoustic radiation; i.e., the flow of compressible gases over the irregular edge of the transitional M6NTC nozzle-wall boundary layer generates weak Mach waves, which radiate into the freestream and are sensed as acoustic disturbances (pressure fluctuations) by the hot wire.

Because evidence of acoustic radiation exists for $Re_\infty = 10.04 \times 10^6$/m at the center of the nozzle exit, the focus of the present research was limited to the BVO case with Re_∞ in the range of $7.87–10.04 \times 10^6$/m. The oscillatory behavior of the rms signal for $Re_\infty > 9.84 \times 10^6$/m was not investigated because this condition was beyond the useful operating range of the facility.

Mean-Flow Measurements

The mean-flow measurements consist of Mach number data that were reduced from the pitot pressure data as previously described. All Mach number data were conducted at a stagnation temperature of 177 ± 2°C with BVO. Note that the variations in Re_∞ were accomplished by varying stagnation pressure for all data presented henceforth.

Figure 4 shows the Mach number contours over the centerline X-Y plane for $Re_\infty = 7.87$ and 10.04×10^6/m. Outside of the approximately uniform flow region, there exist steep Mach number gradients that render the flow unacceptable for most research applications. (The data in Fig. 4 have been spatially low-pass filtered to produce a smooth, detailed contour map.) For $73.05 \lesssim X \lesssim 101.00$ cm, the mean Mach number is approximately 5.91, and this will be considered the reference Mach number of the M6NTC. Figure 4 shows that the nozzle achieves the reference Mach number at $X = 52.73$ cm compared to $X = 46.63$ cm reported for the preplating case.[14] In addition, the overall increase in Mach number as Re_∞ increases confirms the expected thinning of the nozzle-wall boundary layer.

All data presented in Fig. 4 are within 1.4% of the mean Mach number, $M = 5.91$, and this maximum 1.4% deviation, i.e., ± 0.08 M, is used here to define the region of uniform flow. The angle of the 5.85–5.91 contours with respect to the X axis for $55.27 < X < 73.05$ cm compares well with α of the mean Mach number of the freestream flow (see Fig. 4a). Hence, for the current discussion, the uniform nozzle flow begins at $X = 52.73$ cm and is bounded by characteristic lines that may be extrapolated to the nozzle exit.

For the region exterior to the nozzle, uniform flow is maintained inside a line inclined at $\beta \sim 22$ deg extending from the nozzle exit

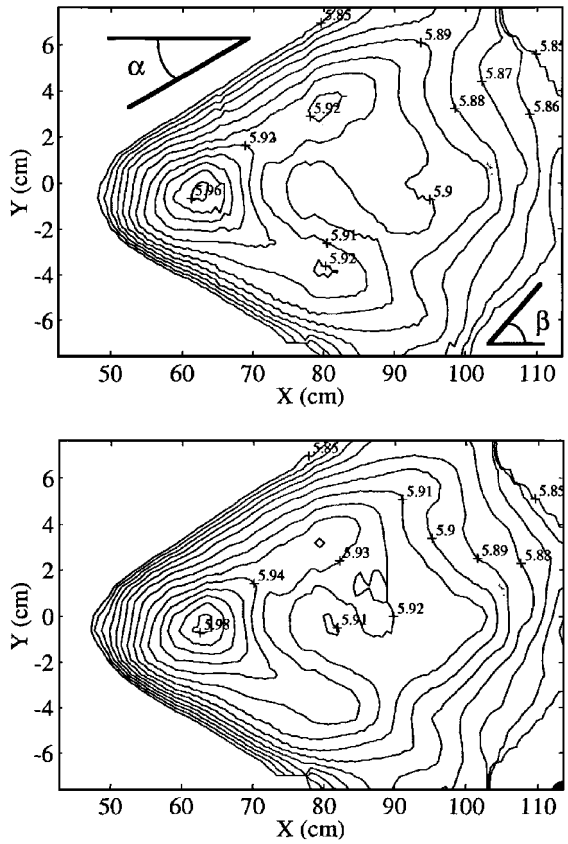

Fig. 4 Mach number contours at a) $Re_\infty = 7.87 \times 10^6$/m, contour increment = 0.01 and b) $Re_\infty = 10.04 \times 10^6$/m, contour increment = 0.01.

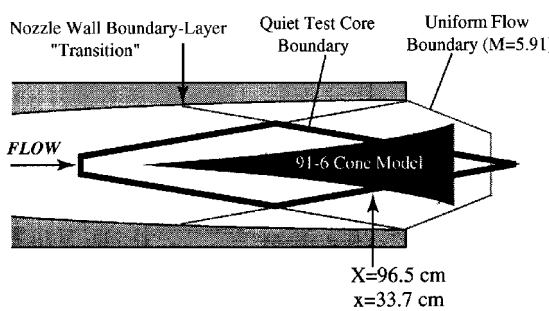

Fig. 5 M6NTC with cone model, $Re_\infty = 9.35 \times 10^6$/m.

to the centerline (see Fig. 4a). The bounding lines of this region are determined by the back pressure of the nozzle because the flow is overexpanded and the bounding lines are generally parallel to the exit shock. Particularly striking in Fig. 4 is the blunted region at $X \sim 52.73$ cm where sharp-tipped contours would be expected and have been presented in the past[10,14] as well as the smooth 1.2% overshoot in M centered at $X = 38.10$ cm. The nozzle design procedure was iterative whereby an inviscid code solution for the nozzle contour was coupled to a viscous code. It is thought that the nozzle-wall boundary layer is not behaving as predicted, which results in the blunting of the M contours and the subsequent M overshoot as a first-order effect. Figure 5 shows the limits of the uniform flow boundary in the M6NTC that are valid for the range of Re_∞ investigated. (The 91-6 cone model referred to in Fig. 5 was used in the hypersonic boundary layer stability study discussed in Ref. 18.)

To investigate possible mean flow asymmetry in the X-Y plane of the nozzle, surveys were conducted at locations $Z = 3.81$ cm above and $Z = -3.81$ cm below the centerline plane at $Re_\infty = 9.35 \times 10^6$/m. The percent difference in Mach number between the two planes is plotted in Fig. 6. Regions of significant Mach number

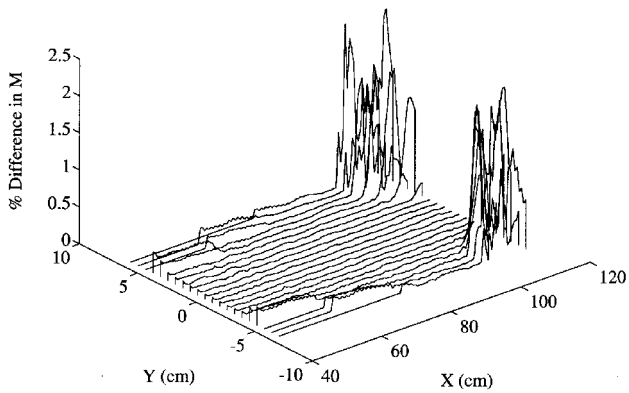

Fig. 6 Percent difference in M between the $Z = 3.81$ and -3.81 cm planes.

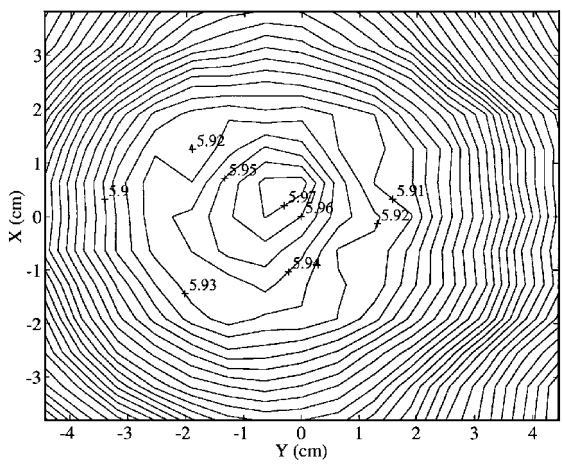

a) $X = 62.89$ cm

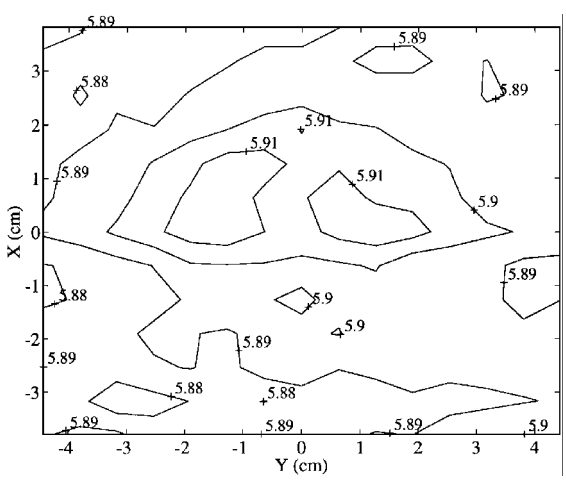

b) $X = 93.37$ cm

Fig. 7 M contours.

difference exist near the exit shock and are outside the uniform flow region defined in Fig. 5. Excluding this region, the symmetry of the flow is well maintained with a much less than 1% difference in Mach number.

The data in Fig. 6 at $Re_\infty = 9.35 \times 10^6$/m confirm symmetry in the X-Y plane, but further data were acquired to verify the axisymmetric nozzle flow. The data in Fig. 7 at $Re_\infty = 9.35 \times 10^6$/m show development of the flow for different Y-Z planes. In the $X = 62.89$ cm locations, the flow is slightly off center but the extent of the asymmetry at any given radius is within 1% of the mean Mach number for that radius. Furthermore, for $X > 93.37$ cm, the entire region investigated is well within 1% of the mean Mach number.

In conclusion, it has been found that the M6NTC has a large region of uniform flow. The development of this uniform flow occurs in an axisymmetric manner and extends downstream of the exit. The uniform flow boundary defined in Fig. 5 may therefore be rotated about the nozzle centerline to define the practical uniform flow volume of the M6NTC.

Unsteady-Flow Measurements

All hot-wire data presented are uncalibrated. Subsequent CVA calibration procedures[16] developed after the conclusion of this investigation have shown that the sensitivities of the test hot wires are approximately constant for a fixed wire voltage over the limited range of tunnel conditions investigated. Because all data sets were acquired at a fixed wire voltage and stagnation temperature fluctuations are assumed to be negligibly small, the rms amplitude measurements may be assumed to linearly approximate the mass-flow fluctuations. The prototypical nature of the CVA precluded a rigorous compressible flow error analysis; hence, the rms amplitudes presented provide a qualitative overview of the Mach wave radiation.

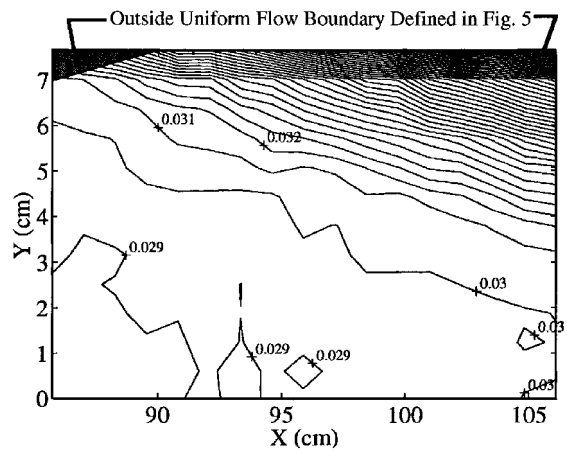

a)

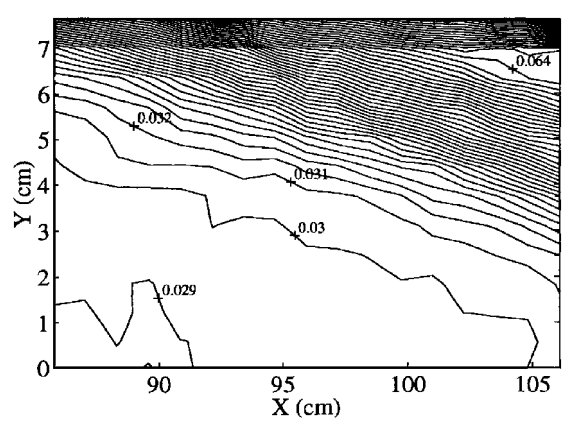

b)

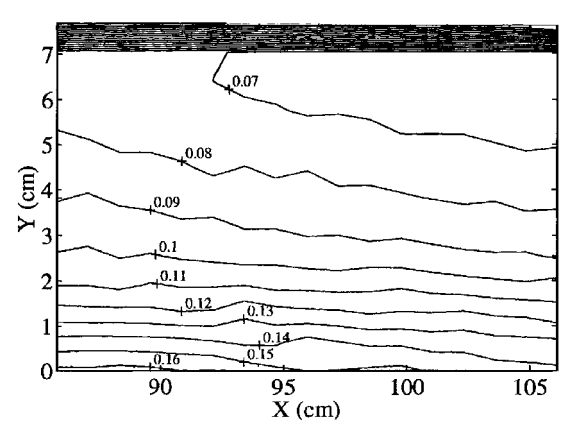

c)

Fig. 8 RMS contours at a) $Re_\infty = 7.87 \times 10^6$/m, contour increment = 0.001; b) $Re_\infty = 9.35 \times 10^6$/m, contour increment = 0.001; and c) $Re_\infty = 11.48 \times 10^6$/m, contour increment = 0.01.

Figure 8 shows the contours of constant rms amplitude for $Re_\infty =$ 7.87, 9.35, and 11.48 $\times 10^6$/m in the region near the exit of the nozzle. Only a small portion of the region investigated lies outside the region of uniform flow (see Fig. 8a). In all cases except $Re_\infty =$ 11.48 $\times 10^6$/m, the disturbance amplitude map contains an extensive region where reasonably straight contours are Mach lines of the freestream flow. Because the entropy and vorticity modes follow streamlines and not characteristics, the coincidence of the contours with α implies that the disturbances are acoustic in nature and are generated by acoustic sources on the nozzle wall; i.e., the nozzle wall boundary layer is becoming turbulent and sound mode noise is radiating into the otherwise quiet freestream. (For brevity, this sound mode noise is referred to as acoustic radiation for the remainder of this paper.) The amplitude of the disturbances radiating from the nozzle wall increases with Re_∞ for a fixed X location. This Re_∞ dependency suggests that the transition of the nozzle-wall boundary layer is not due to a roughness-induced bypass transition mode but is more likely due to the natural development of Görtler vortices.[14]

In Fig. 3 the rms amplitude slightly increased at $Re_\infty = 10.04 \times 10^6$/m from the noise level value at $Re_\infty = 9.35 \times 10^6$/m. The data in Fig. 8b show that acoustic radiation exists at $Re_\infty = 9.35 \times 10^6$/m but is not evident at the centerline of the nozzle exit ($X = 101.0$ cm, $Y = 0$). Once Re_∞ has increased to 10.04×10^6/m, the transition front has moved forward so that disturbances radiating from several independent acoustic sources around the periphery of the nozzle wall impinge on the hot-wire sensor and the slight increase in rms shown in Fig. 3 is realized. (Note that the amplitudes of Figs. 3 and 8 are not identical because different hot-wire probes were used.) For values of $Re_\infty > 10.04 \times 10^6$/m, the transition front has moved further forward and the hot-wire located at the center of the nozzle exit measures the signal associated with numerous and potentially interacting acoustic radiation. As Re_∞ increases further, the disturbance field takes on a nearly radial character where the amplitude of the acoustic radiation depends primarily on Y and characteristic lines in the disturbance map can no longer be discerned. Such is the case of $Re_\infty = 11.48 \times 10^6$/m in Fig. 8c, and this would be the expected acoustic radiation field in a conventional axisymmetric high-speed wind tunnel. From this discussion, it is evident that data on the centerline of the nozzle present only a small portion of the transition process.

If the rms data nearest the nozzle wall are plotted for a variety of Re_∞ a clear Reynolds number dependency is observed. In Fig. 9, the rms amplitude data for $Y = 7.62$ cm, $85.75 \leq X \leq 101.0$ cm over a range of Re_∞ has been plotted vs Re_X in Fig. 9a based on the X length scale and vs Re_V in Fig. 9b based on a V-length scale originating 37.49 cm downstream of the nozzle throat. The rms data collapse to a single line in the latter case; hence, $X = 37.49$ cm may be considered a virtual origin of the fluctuating nozzle-wall boundary layer. No apparent geometric aberration was found for this virtual origin; e.g., a joint location or other such flow-perturbing roughness site. The Reynolds number relationship evidently applies only in the region of initial acoustic radiation generation (i.e., $Re_\infty \leq 10.04 \times 10^6$/m). At higher Re_V, the amplitude of the radiated acoustic disturbances tends to reach a constant level because the boundary layer becomes fully turbulent, the flow becomes saturated with disturbances (see Fig. 8c), and a unique relationship can no longer be discerned.

From the data in Fig. 9, the nozzle-wall disturbances become measurable when Re_V exceeds 3.30×10^6; i.e., $X < 65.68$ cm for a stagnation pressure of 896 kPa, which differs from the $X = 90.83$ cm reported in a Ref. 11 for nozzle-wall transition under similar flow conditions. This discrepancy is explained by the different disturbance levels used to define noisy flow, with the present method relying on a more sensitive criterion: an increase in disturbance amplitude above the noise level.

The method of quantifying the performance of a quiet nozzle requires computing the variation of $Re_{\Delta X}$ with Re_∞. The length of the quiet test core, ΔX, is shown in Fig. 1 and is bounded by the start of uniform flow on the upstream end and by initial acoustic radiation (or noisy flow) on the centerline at the downstream end. In Fig. 10, $Re_{\Delta X}$ for the present investigation has been computed and plotted with previous nozzle data (acquired before the plating process) and the theoretical estimation for $N_G = 7.5$ (Ref. 14). By

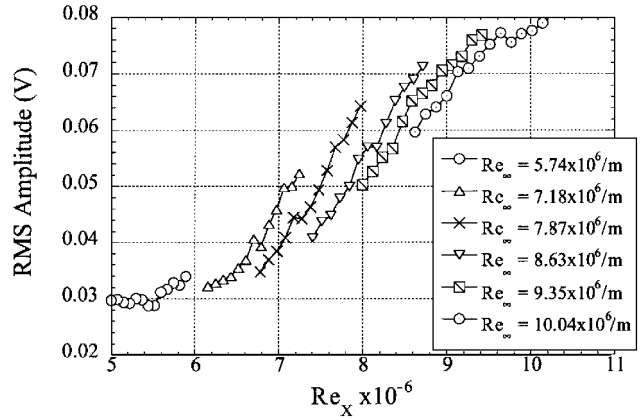

a) Origin at $X = 0$ cm

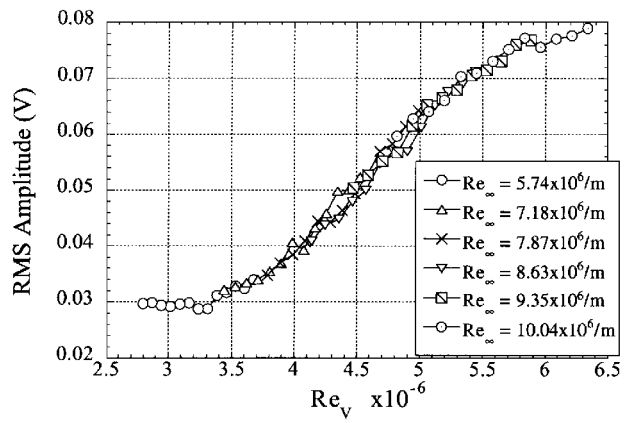

b) Origin at $X = 37.49$ cm

Fig. 9 Re_X.

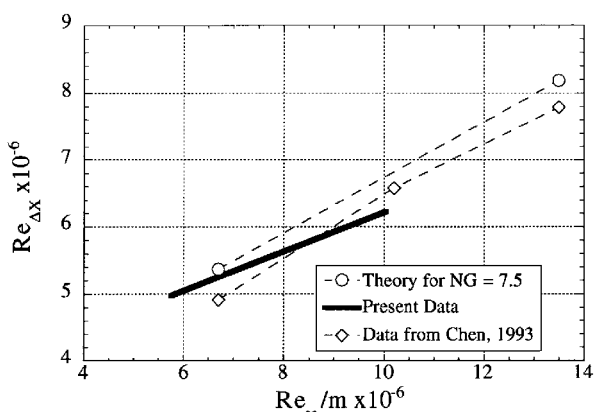

Fig. 10 $Re_{\Delta X}$ variation with Re_∞.

using the virtual origin found in Fig. 9, the transition point of the nozzle-wall boundary layer may be defined at $Re_{VT} = 3.3 \times 10^6$. For the present data, the following relationship was found for $Re_{\Delta X}$ over the range of Re_∞ investigated:

$$Re_{\Delta X} = 0.956\, Re_\infty + Re_{VT}$$

The present data in Fig. 10 show a higher $Re_{\Delta X}$ at $Re_\infty = 6.56 \times 10^6$/m than the earlier investigation but a lower $Re_{\Delta X}$ at $Re_\infty = 9.84 \times 10^6$/m. Both sets of data compare well with the theoretical $Re_{\Delta X}$ based on the growth of Görtler vortices. It is concluded that the nozzle refurbishment conducted between the initial calibration and the present investigation has not significantly altered the performance of the nozzle for $Re_\infty < 10.04 \times 10^6$/m.

Overall, the acoustic radiation zone of influence is limited. The $Re_{\Delta X}$ relationship given earlier and the uniform flow region found

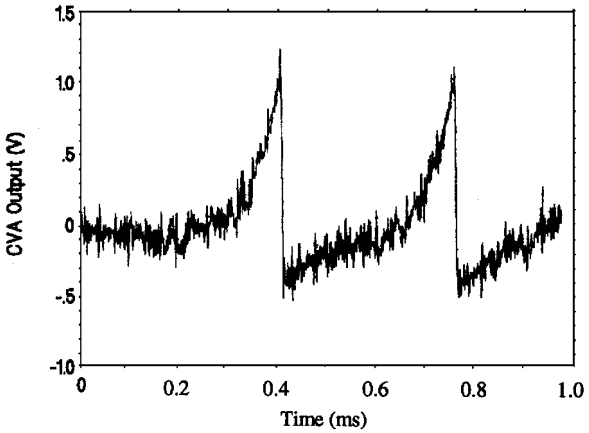

Fig. 11 Typical data spikes indicative of sound mode disturbances.

previously may be used to define the extent of quiet flow. For the case of $Re_\infty = 9.35 \times 10^6$/m in Fig. 5, the quiet flow boundary is defined as the intersection of the uniform flow region with the low-freestream disturbance region. As a practical application of these data, the cone model used in later stability research[18] is shown in its test position and the extent of the quiet flow region is apparent.

The character of the large acoustic disturbances radiating from the nozzle wall is shown in the time trace data of Fig. 11. The probe was fixed at the center of the nozzle exit with $Re_\infty = 10.76 \times 10^6$/m. These intermittent data spikes were reported earlier[11] for a variety of Re_∞ and it was shown that the intermittency increases with Re_∞. This increase results in the rms amplitude increase shown in Figs. 3 and 8 as well as that presented in Fig. 26 of Ref. 10. As shown in Fig. 11, these acoustic disturbance spikes are characterized by a region of exponential growth, a sudden amplitude decrease, and an exponential recovery to the baseline level. The instantaneous change in spike amplitude is thought to represent a discontinuous change in flow properties, not unlike a weak traveling shock wave separating regions of incrementally higher and lower pressure. It was noticed that the amplitude of the acoustic disturbances changes with location. The spikes tend to be more negative-going near the nozzle wall and are more positive-going (as in Fig. 11) near the nozzle centerline.

Conclusions

From this investigation, there have been several important findings related to the performance of the M6NTC. The nozzle was found to contain a significant volume of uniform flow with $M = 5.91$ starting at $X = 52.73$ cm and extending beyond the nozzle exit. The acoustic radiation (sound mode) was primarily responsible for generation of freestream disturbances in the M6NTC. These acoustic disturbances followed Mach lines into the freestream and have the spectral content of disturbances found in conventional high-speed tunnels. For regions near the nozzle wall, the disturbance amplitude is Reynolds number dependent based on a virtual origin 37.49 cm downstream of the nozzle throat. Overall, the laminar-flow control techniques used in development of the M6NTC have produced an extensive region of quiet flow suitable for high-speed stability research where the detrimental effects of freestream disturbances may be minimized.

Acknowledgments

This work was supported by NASA Grants NCC-1-180 (A.E.B.) and NCC-1-183 (J.T.L.) from NASA Langley Research Center. The authors would like to thank N. Chokani and G. Selby for their technical review of this work. The CVA system was developed by Tao Systems. Special thanks are extended to G. R. Sarma of Tao Systems for providing assistance with the CVA. We also thank Fang-Jeng Chen for sharing unpublished results (Jan. 1995).

References

[1]Morkovin, M. V., "On Transition Experiments at Moderate Supersonic Speeds," *Journal of the Aeronautical Sciences*, Vol. 24, No. 7, 1957, pp. 480–486.

[2]Morkovin, M. V., "On Supersonic Wind Tunnels with Low Free-Stream Disturbances," *Journal of Applied Mechanics*, Vol. 26, Sept. 1959, pp. 319–324.

[3]Laufer, J., "Aerodynamic Noise in Supersonic Wind Tunnels," *Journal of the Aeronautical Sciences*, Vol. 28, No. 9, 1961, pp. 685–692.

[4]Laufer, J., "Some Statistical Properties of the Pressure Field Radiated by a Turbulent Boundary Layer," *Physics of Fluids*, Vol. 7, No. 8, 1964, pp. 1191–1197.

[5]Pate, S. R., and Schueler, C. J., "Radiated Aerodynamic Noise Effects on Boundary-Layer Transition in Supersonic and Hypersonic Wind Tunnels," *AIAA Journal*, Vol. 7, No. 3, 1969, pp. 450–457.

[6]Pate, S. R., "Measurements and Correlations of Transition Reynolds Numbers on Sharp Slender Cones at High Speeds," *AIAA Journal*, Vol. 9, No. 6, 1971, pp. 1082–1090.

[7]Kovasnay, L. S. G., "Turbulence in Supersonic Flow," *Journal of the Aeronautical Sciences*, Vol. 20, No. 10, 1953, pp. 657–682.

[8]Laufer, J., "Factors Affecting Transition Reynolds Numbers on Models in Supersonic Wind Tunnels," *Journal of the Aeronautical Sciences*, Vol. 21, No. 7, 1954, pp. 497, 498.

[9]Beckwith, I. E., Chen, F.-J., Wilkinson, S. P., Malik, M. R., and Tuttle, D., "Design and Operational Features of Low-Disturbance Wind Tunnels at NASA Langley for Mach Numbers from 3.5 to 18," AIAA Paper 90-1391, June 1990.

[10]Wilkinson, S. P., Anders, S. G., Chen, F.-J., and Beckwith, I. E., "Supersonic and Hypersonic Quiet Tunnel Technology at NASA Langley," AIAA Paper 92-3908, July 1992.

[11]Wilkinson, S. P., Anders, S. G., Chen, F.-J., and White, J. A., "Status of NASA Langley Quiet Flow Facility Developments," AIAA Paper 94-2498, June 1994.

[12]Beckwith, I. E., "Development of a High Reynolds Number Quiet Tunnel for Transition Research," *AIAA Journal*, Vol. 13, No. 3, 1975, pp. 300–306.

[13]Anders, J. B., Stainback, P. C., Keefe, L. R., and Beckwith, I. E., "Fluctuating Disturbances in a Mach 5 Wind Tunnel," *Ninth Aerodynamic Testing Conference* (Arlington, Texas), AIAA, New York, 1976.

[14]Chen, F.-J., and Wilkinson, S. P., "Görtler Instability and Hypersonic Quiet Nozzle Design," *Journal of Spacecraft and Rockets*, Vol. 30, No. 2, 1993, pp. 170–175.

[15]Stetson, K. F., Thompson, E. R., Donaldson, J. C., and Siler, L. G., "On Hypersonic Transition Testing and Prediction," AIAA Paper 88-2007, June 1988.

[16]Lachowicz, J. T., and Chokani, N., "Hypersonic Boundary Layer Stability Experiments in a Quiet Wind Tunnel with Bluntness Effects," NASA CR-198272, Jan. 1996.

[17]Lachowicz, J. T., Chokani, N., and Wilkinson, S. P., "Hypersonic Boundary Layer Stability over a Flared Cone in a Quiet Tunnel," AIAA Paper 96-0782, Jan. 1996.

[18]Blanchard, A., and Selby, G., "An Experimental Investigation of Wall Cooling Effects on Hypersonic Boundary-Layer Stability in a Quiet Wind Tunnel," NASA CR-198287, Feb. 1996.

[19]Doggett, G. P., "Hypersonic Boundary Layer Stability on a Flared Cone at Angle of Attack," Ph.D. Dissertation, Mechanical and Aerospace Engineering Dept., North Carolina State Univ., Raleigh, NC, May 1996.

[20]Kline, S. J., and McClintock, F. A., "Describing Uncertainties in Single-Sample Experiments," *Mechanical Engineering*, Vol. 75, Jan. 1953, pp. 3–8.

[21]Sarma, G. R., "Analysis of a Constant Voltage Anemometer Circuit," Inst. of Electrical and Electronics Engineers/Instrumentation and Measurement Technology Conf., IEEE 93CH3292-0, Irvine, CA, May 1993.

[22]Mangalam, S. M., Sarma, G. R., Kuppa, S., and Kubendran, L. R., "A New Approach to High-Speed Flow Measurements Using Constant Voltage Anemometry," AIAA Paper 92-3957, July 1992.